JOURNAL OF VIROLOGY, Apr. 1992, p. 2251–2260
0022-538X/92/042251-10$02.00/0

Vol. 66, No. 4

VPg Gene Amplification Correlates with Infective Particle Formation in Foot-and-Mouth Disease Virus

MATTHIAS M. FALK,[1]† FRANCISCO SOBRINO,[2] AND EWALD BECK[3]*

Departamento de Sanidad Animal, Centro de Investigatión y Tecnologia, Instituto Nacional de Investigationes Agrarias, Madrid, Spain,[2] and Zentrum für Molekulare Biologie Heidelberg, Universität Heidelberg, Heidelberg,[1] and Biochemisches Institut am Klinikum der Universität Giessen, Friedrichstrasse 24, D-6300 Giessen,[3] Germany

Received 14 August 1991/Accepted 17 December 1991

In order to analyze the function of VPg amplification in aphthoviruses, we have undertaken the first mutational analysis of the repetitive VPg-coding region using an improved foot-and-mouth disease virus (FMDV) cDNA clone from which infective viral RNA was synthesized. A set of VPg mutants was constructed by site-directed mutagenesis which includes different VPg deletion mutations, a VPg insertion mutation, and amino acid residue replacement mutations that interfere with binding of the VPg protein to the viral RNA and with its proteolytic processing. Our results revealed that an amazing flexibility in the number of VPgs is tolerated in FMDV. Optimal viability is given when three VPgs are encoded. Deletion as well as insertion of one VPg gene still resulted in infective particle production. Infective particle formation was observed as long as one VPg remained intact. No obvious differences in the individual VPg molecules with regard to their promoting viral RNA synthesis were observed, indicating that all three VPgs can act equally in FMDV replication. Mutant polyprotein processing was comparable to that of the wild-type virus. However, VPg mutants showed reduced viral RNA synthesis levels after infection. The levels of viral RNA synthesis and infective particle formation were found to correlate with the number of functional VPgs left in the mutant virus. These findings suggest a direct VPg gene dosage effect on viral RNA synthesis, with a secondary effect on infective particle formation.

The foot-and-mouth disease virus (FMDV) genome is a messenger-sense, single-stranded RNA genome approximately 8,500 nucleotides in length with characteristics shared by other members of the picornavirus family. The 5′ end of picornavirus genomic RNA is covalently linked to a small (2.4-kDa) virus-encoded protein termed VPg (viral genome-linked protein) (reviewed in reference 48; also see reference 36) or polypeptide 3B (35). The VPg gene is located in the P3 region of the viral genome, where it is flanked by the genes for polypeptide 3A, a protein proposed to be the membrane anchor of the picornavirus replication complex (40, 44), and the viral proteinase $3C^{pro}$. Other viral proteins associated with the membrane-bound picornavirus replication complex were identified as polypeptide 2C, which is involved in guanidine resistance (30, 39), and the viral RNA polymerase $3D^{pol}$.

Since VPg was found to be linked to all newly synthesized viral RNAs, it has been proposed that VPg, a VPg-precursor protein (3AB), or an uridylylated form of VPg acts as a primer to initiate picornavirus RNA synthesis (5, 9, 25, 42, 46, 47). Although poliovirus replication has been extensively investigated (for reviews, see references 11, 24, 29, 31, 34, and 49 and references cited therein), this process remains poorly understood.

In the past, two different models have been proposed to explain the mechanisms involved in picornavirus RNA replication and the linkage of VPg to viral RNA. In one model, VPg is proposed to act as a primer for plus- and minus-strand RNA synthesis. This model is supported by the fact that, for instance, VPg can be elongated into VPg-pUpU (44). The other model proposes VPg-independent, self-priming minus-strand RNA synthesis after the addition of several U residues to the poly(A) tail of the viral RNA by terminal uridylyl transferase. This model is supported by, for instance, the isolation of viral RNA twice the length of poliovirion RNA in an in vitro replication system (50).

New data, obtained by several groups, support a hypothesis that minus- and plus-strand RNA synthesis could take place in two different ways (29). Reuer et al. (31) showed that mutation of the RNA-linking tyrosine residue, conserved at position 3 of all VPgs, completely abolished viral RNA synthesis. This supports a model of VPg-primed plus- and minus-strand RNA synthesis as originally proposed by Wimmer (47) and his coworkers (27).

On the other hand, self-catalyzed linkage of VPg to minus-strand poliovirus RNA in the absence of any additional factors such as polymerase, host factor, and ribonucleoside triphosphates was found by Tobin et al. (45) and Flanegan et al. (10). These findings would support a VPg-independent template priming mechanism for minus-strand RNA synthesis (50). A model for the covalent attachment of VPg by nucleophilic attack involving a specific sequence in the 3′ terminal region of the viral genome is proposed by these investigators (10, 45).

Finally, Andino et al. (2) verified a computer-predicted cloverleaf structure at the 5′ end of poliovirus RNA that forms a functional ribonucleoprotein complex which consists of a cellular protein, viral proteinase $3C^{pro}$, and the viral polymerase $3D^{pol}$. Mutations altering the cloverleaf structure in the positive strand but not in the negative strand were lethal to the virus. Giachetti and Semler (15) characterized a poliovirus mutant defective in both in vitro uridylylation of VPg and in vivo synthesis of plus-strand viral RNAs, while minus-strand RNA synthesis was not affected. These observations also strongly support two fundamentally different ways to initiate picornavirus positive- and negative-strand RNA synthesis.

In addition to its role in genome replication, VPg is proposed to be involved in encapsidation of viral RNA (27,

* Corresponding author.
† Present address: Department of Molecular Biology, The Scripps Research Institute, La Jolla, CA 92037.

28) because exclusively RNA-carrying, covalently linked VPg was found in virions, although the same RNA without covalently linked VPg is a major species in the infected cell (28).

Reuer et al. (32) and Kuhn et al. (23) reported considerable flexibility in several positions of the amino acid sequence of VPg. As long as tyrosine 3 was left intact, viral RNA synthesis occurred and VPg was linked to the viral RNA (10, 32), although no viable virus could be observed. This finding strongly suggests an additional VPg-dependent step in poliovirus replication following RNA synthesis.

The role of VPg in FMDV seems to be more complex than its role in the other picornaviruses. Sequence analysis of the FMDV genome revealed three VPg genes arranged in tandem and designated VPg1, VPg2, and VPg3 (12), an astonishing redundancy considering the small genome size. All other picornavirus groups have only one VPg-coding region. The three VPg genes are related but distinctly different from one another and were found in an equimolar ratio in virions, suggesting equivalent functions in vivo (21). Since no specialized function of each individual VPg was found, a selective advantage for a high VPg gene copy number in FMDV was presumed (12).

To study the dependence of the FMDV replication on the three VPg genes, we constructed a set of VPg mutants consisting of VPg deletion mutants, a VPg insertion mutant, and different amino acid residue replacement mutants. The viability of the mutant constructs was investigated by transfecting BHK G21 cells and IBRS2 cells. Mutants were further characterized by (i) determining the virus titers of the individual mutants, (ii) detecting viral polyprotein processing in vitro and in vivo by using specific antisera directed against P3 polypeptides, and (iii) by measuring viral RNA synthesis levels following infection.

MATERIALS AND METHODS

Infectious recombinant FMDV full-length cDNA clone. VPg mutations were introduced into the FMDV genome by using a new infectious cDNA clone, pSP65FMDVpolyC, a derivative of our first full-length cDNA plasmid, pFMDV-YEP-polyC (51). Details of the construction and properties of this clone will be described elsewhere (8). Essentially, in this plasmid the yeast shuttle vector part of pFMDV-YEP-polyC (51) has been replaced by the RNA expression vector pSP65 (26) and the poly(C)-coding sequence was elongated to 39 nucleotides.

Construction of VPg mutants. Nucleotide-specific mutations, for instance, VPg deletions and amino acid residue exchanges, were introduced into the repetitive VPg-coding region by site-directed mutagenesis in combination with polymerase chain reaction (PCR) technology basically as described by Higuchi et al. (19) and in combination with standard PCR protocols (20). Phenylalanine (F) exchange mutants were introduced by using sets of primers containing the F codon UUU instead of the tyrosine (Y) codon UAC. VPg deletion mutants were constructed by using primer sets that loop out the individual VPg-coding region. Mismatch-primer lengths ranged from 21 to 26 nucleotides, and primers for deletion loop mutagenesis were 30 nucleotides long. Two flanking primers complementary to plus- and minus-strand FMDV cDNA upstream of the *Xba*I site at position 5418 and downstream of the *Sac*I site at position 5809 (13) were used in all reactions to prime complementary-strand synthesis. To reduce the introduction of random point mutations by *Taq* polymerase, up to 500 ng of template DNA was used in each reaction in combination with only 15 amplification cycles. PCR-amplified fragments were cleaved with *Xba*I and *Sac*I and were used to replace the equivalent restriction fragment in the plasmid pSp5.1-6.3, which contains the FMDV genome from nucleotide 5149 (*Eco*RI) to position 6296 (*Pst*I). The absence of additional mutations in the PCR-amplified products was verified by DNA sequencing with a T7 sequencing kit (Pharmacia, LKB Biotechnology Inc., Uppsala, Sweden). The VPg mutations were then introduced into the recombinant infectious full-length cDNA clone (pSP65FMDVpolyC) by replacing the corresponding *Eco*RI-*Pst*I fragment of the FMDV cDNA.

An additional VPg1 was introduced into the viral cDNA by cloning two complementary 69-nucleotide oligonucleotides into the *Xho*I site (position 5557) within the VPg1-coding region. The correct orientation of the introduced synthetic VPg gene was checked by sequencing. The resulting FMDV mutant, +VPg1+, contained an in-frame duplication of the VPg1-coding region.

To ensure that no reduction in the length of the poly(C) region occurred during amplification of the full-length cDNA clone in *Escherichia coli* (8), the size of the poly(C) tract was verified in every mutant cDNA batch used. All molecular-cloning techniques were performed by standard methods (37).

In vitro transcription and translation. In vitro transcription was performed essentially as described previously (26). Large amounts of synthetic full-length RNA (up to 10-fold excess over DNA) were obtained by transcribing linearized plasmid DNA with SP6 RNA polymerase (USB Corp., Cleveland, Ohio). About 2 μg of RNA was translated in 50 μl of rabbit reticulocyte lysate (Amersham Buchler, Braunschweig, Germany) in the presence of 20 μCi of [^{35}S]methionine (>1,000 Ci/mmol; Amersham). Reaction mixtures were incubated at 30°C for 1 h and then heated to 37°C and further incubated. At 30 min, 1-, 2-, 4-, and 6-h aliquots were removed and analyzed.

Cells and viruses. For transfections, virus propagation and titration BHK G21 (BHK) or IBRS2 (a swine-derived cell line) cell monolayers were used. Viral RNA and protein synthesis were analyzed for BHK cells only. Both cell lines were cultivated in Dulbecco's modified Eagle's medium (DMEM) supplemented with 5% newborn calf serum as described previously (7).

The calcium phosphate coprecipitation method, essentially as described by Kingston (22) without DEAE-dextran treatment or glycerol boost, was used for RNA transfections of tissue culture cells. Semiconfluent BHK or IBRS2 cell monolayers, split 1 day prior to transfection into 10-cm-diameter cell culture dishes (approximately 2×10^6 to 4×10^6 cells), were transfected with approximately 1 μg of synthetic RNA. Plaques of typical shape, formed by rounded, infected cells, were observed between 1 and 3 days posttransfection. Mutant RNAs were considered nonviable if no cytopathic effect was detected in several independent transfections 4 days posttransfection. Mutant viruses were amplified by one transfer of virus-containing transfection medium onto new cell monolayers. After cell lysis, virus-containing medium was removed and deep-frozen to serve as virus stock. Since mutant viruses showed a reduced ability to grow in BHK cells under 0.7% agar overlay, resulting in hardly visible plaque formation, all virus titers were additionally measured by serial dilutions. Aliquots of the individual dilution steps were added to confluent BHK cell monolayers growing in 96-well tissue culture plates. This procedure resulted in plaques formed by rounded, infected

cells clearly visible under the microscope after 1 day of incubation. Wild-type (*wt*) viruses, derived from several field isolates ($O1_{Kaufbeuren}$, $O1_{Murchin}$, O_{Israel}) and recombinant full-length clone-derived virus (rFMDV-C_{39}), showed comparable titers as determined either by plaque assay using 0.7% agar overlay or by serial dilution of virus stocks. To determine the virus titers achieved by the individual FMDV mutants under comparable conditions, semiconfluent BHK cell monolayers (5×10^5 cells) growing in 6-cm-diameter tissue culture dishes were infected with 10^4 PFU in 5 ml of DMEM. After complete lysis of the cell monolayers, the medium was removed and cleared by centrifugation and the virus titers were determined by serial dilution steps as described above.

Analysis of virus-specific proteins in infected cells. Semiconfluent monolayers of BHK cells grown in 6-cm-diameter tissue culture dishes (approximately 5×10^5 cells) were infected at a multiplicity of infection of 1. Infection was allowed to proceed for 1 h at 37°C. Then the medium was replaced by 2 ml of DMEM without methionine (GIBCO/BRL, Eggenstein, Germany), and 100 μCi of [^{35}S]methionine (>1,000 Ci/mmol; Amersham) was added per dish. At 2, 2.5, 3, 3.5, 4, and 6 h, labeling was stopped by washing with ice-cold 1× phosphate-buffered saline (PBS) and lysing the cells in 0.5 ml of freshly prepared RIPA buffer (150 mM NaCl, 1% Nonidet P-40, 0.5% sodium deoxycholate, 0.1% sodium dodecyl sulfate [SDS], 50 mM Tris-HCl, pH 7.5). Extracts were incubated for 10 min at 70°C to denature virus particles. To increase the amount of soluble viral proteins that are predominantly bound to membranes in the viral replication complex (16, 43), extracts were frozen and then thawed and sonified for 10 s. Insoluble membrane debris was pelleted by centrifugation. Aliquots of the cleared supernatants were used for immunoprecipitation reactions of viral polypeptides.

Immunoprecipitation of viral polypeptides. FMDV-specific antisera used were raised against bacterially synthesized fusion proteins constructed by Strebel et al. (41) in our laboratory. Immunoprecipitations of in vitro and in vivo synthesized FMDV polypeptides were performed essentially as described previously (41) by standard methods (17). To reduce coprecipitation of unspecific polypeptides, 15 μl of translated reticulocyte lysate or 100 μl of cell lysate was diluted with 1 ml of RIPA buffer and heated at 70°C for 10 min. After cooling to room temperature, 3 μl of antiserum and preswollen protein-A Sepharose was added to the reaction mixture. Reaction mixtures were incubated for 1 h at 4°C with vigorous shaking. Immunoprecipitation complexes were washed 3 times each with 1 ml of RIPA buffer prior to solubilization in sample buffer. Immunoprecipitated proteins were separated by 12.5% SDS-polyacrylamide gel electrophoresis.

Labeling of infected cells with [^{3}H]uridine. Total viral RNA synthesis was assayed essentially according to a method described by Helenius et al. (18). BHK cells were grown on 16-mm-diameter glass coverslips placed into 6-cm-diameter cell culture dishes (seven per dish; approximately 5×10^4 cells per coverslip). Coverslips were previously washed in ethanol and rinsed in 1× PBS containing 0.1% gelatin. After 24 h, exponentially growing cells were washed and infected with 1.5 ml of virus solution in DMEM (2 PFU per cell). Since some mutant viruses reached only low titers (about 10^5 PFU/ml for the double-tyrosine mutants [see Fig. 2]), virus particles were first concentrated by using Centricon 100 microconcentrators (Amicon, W. R. Grace & Co., Witten, Germany), following the instructions of the manufacturer. After incubation for 1 h at 37°C with occasional agitation, medium was removed and replaced by 1 ml of fresh DMEM containing 1 μg of actinomycin D per ml to inhibit host cell DNA-directed RNA synthesis (4) and 10 μCi of [^{3}H]uridine per ml (5,6-[^{3}H]uridine, 45 Ci/mmol; Amersham). At indicated times, coverslips were removed, rinsed in 1× PBS, and transferred to 5 ml of ice-cold 10% trichloroacetic acid. The latter step was repeated two times. Finally, the coverslips, with the cells visible as a white layer, were rinsed in ethanol and dried, and the levels of radioactivity were determined by liquid scintillation counting with a polyamine-based scintillant (Quicksafe A; Zinsser Analytic, Frankfurt, Germany).

RESULTS

Threefold VPg gene amplification is no prerequisite for FMDV viability. To analyze whether the VPg triplet is a prerequisite for infectivity of aphthoviruses, we constructed different mutants with complete deletions of VPg1 (ΔVPg1), VPg2 (ΔVPg2), or VPg3 (ΔVPg3) and a VPg insertion mutant (+VPg1+) containing a duplicated VPg1, thus carrying four VPg genes. To investigate the influence of the number of VPg genes on viral RNA synthesis without affecting the overall structure of the viral polyprotein, we constructed, in addition, a set of VPg mutants incapable of priming viral RNA synthesis or being linked to the newly synthesized RNA. Reuer et al. (32) and Flanegan et al. (10) reported that exchange of the conserved linking tyrosine (Y) amino acid residue at position 3 of VPgs into phenylalanine (F) resulted in a protein that could not be uridylylated. VPg Y-to-F exchange mutants of poliovirus were completely defective in synthesis of viral RNA (32).

In analogy, FMDV mutants with either one (VPg1F, VPg2F, and VPg3F) or two (VPg1F/2F, VPg1F/3F, and VPg2F/3F) Y-3-to-F-3 exchanges were constructed, leaving the structure of the viral polyprotein otherwise unaffected (Fig. 1).

To our surprise, all VPg mutants except mutant ΔVPg3 were found to be infectious in BHK and IBRS2 cells. Several mutants showed a strongly reduced viability (Fig. 2). No obvious difference between the two cell lines used was observed, except that transfection and virus growth were generally more efficient in IBRS2 cells. Virus titers of the different VPg mutants in IBRS2 cells did not differ significantly from virus titers in BHK cells. The experiments described here were all carried out with BHK cells.

The life cycles of the recombinant *wt* virus (rFMDV-C_{39}) and of all of the mutant viruses (Fig. 1) were comparable to those of the field-isolated *wt* viruses ($O1_{Kaufbeuren}$, $O1_{Murchin}$, $O1_{Israel}$). A cytopathic effect became visible for all mutants approximately 4 h postinfection. The reduced plaque size of the mutant viruses was not due to a retarded replication cycle but to the lower number of infectious particles produced per cell. This is obvious from the [^{3}H]uridine incorporation kinetics (see Fig. 4) which culminates for all VPg mutants tested at 3 to 3.5 hours postinfection and can also be seen from the individual mutants. After 4 h, processing of the polyprotein of the cDNA-derived *wt* virus is very similar to processing of the mutants (compare, e.g., the anti-E12 and anti-E20 immunoprecipitation lanes of rFMDV-C_{39} with the corresponding lanes of the VPg Y-to-F mutants in Fig. 3).

Virus production correlates with the number of functional VPgs. The efficiency of transfection and virus propagation indicated a reduced viability of VPg mutant constructs but

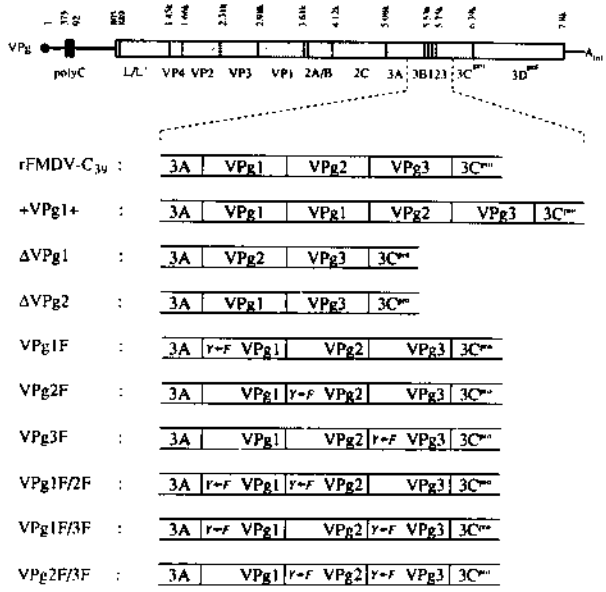

FIG. 1. Schematic representation of the VPg-coding regions of recombinant full-length clone (rFMDV-C_{39}) and VPg mutant viruses of FMDV. The VPg-coding regions of a VPg1 insertion mutant (+VPg1+) encoding four VPg polypeptides, VPg deletion mutants of VPg1 (ΔVPg1) and VPg2 (ΔVPg2), and VPg tyrosine 3-to-phenylalanine 3 exchange amino acid residue mutants (Y→F) are shown. All VPg mutants are based on the recombinant full-length clone pSP65FMDVpolyC (8). The FMDV genetic map is shown on top. The thin line is the nontranslated region, while the boxes are the open reading frame showing the locations of the viral proteins. VPg polypeptide linked to the 5′ end of the viral RNA, poly(C) coding region within the 5′ noncoding region, and poly(A) tail at the 3′ end of the viral genome are also shown. The lengths of the individual genome fragments are indicated above the open reading frame in kilobases according to Forss et al. (13). Both 3B and VPg (35), which are synonymous, are used in this scheme.

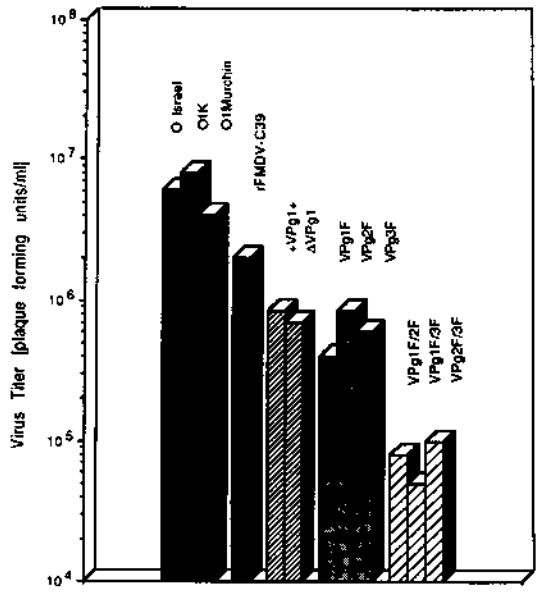

FIG. 2. Virus titers of field isolate-derived *wt* virus strains O_{Israel}, $O1_{Kaufbeuren}$ (O1K), and $O1_{Murchin}$; full-length clone-derived *wt* virus (rFMDV-C_{39}); and VPg mutant viruses determined under comparable conditions. Semiconfluent BHK G21 cell monolayers (5 × 10^5 cells each) were infected with 10^4 infective particles of the respective viruses. After complete lysis of the cells, virus titers were determined by serial dilutions and plaque assay.

no effect on the life cycle length. Therefore, virus titers of the individual mutants and *wt* viruses were determined under comparable conditions, as described in Materials and Methods. The different titers of *wt* and mutant viruses (Fig. 2 and Table 1) can be divided into three groups. Recombinant nonmutated virus (rFMDV-C_{39}) reached a titer of 2 × 10^6 PFU/ml, which is slightly reduced but comparable to the titer of the *wt* viruses $O1_{Kaufbeuren}$, O_{Israel}, and $O1_{Murchin}$. A second group is represented by virus mutants coding for either four VPg polypeptides or only two functional VPgs. Virus titers of this group ranged from 8.5 × 10^5 to 4 × 10^5 PFU/ml (+VPg1+, ΔVPg1, VPg1F, VPg2F, VPg3F) in our assay. Mutants ΔVPg2 and ΔVPg3 behaved differently from the ΔVPg1 mutant because of altered P3 polyprotein precursor processing. The ΔVPg2 mutant has a strongly reduced level of infectivity on BHK and IBRS2 cells. Infective particles were found in only one of five independent transfection experiments, while the ΔVPg3 mutant was never observed to be viable. Additional results obtained for these two mutants are described below. The third group of VPg mutants, represented by viruses coding for only one functional VPg, reached only very low virus titers of between 1 × 10^5 and 5 × 10^4 PFU/ml.

VPg mutations were maintained stably over all passages tested so far. Presence of the exchanged nucleotides in the RNA of the Y-to-F mutants VPg1F, VPg2F, and VPg3F was confirmed by sequencing primary cDNA (3) derived from the RNA of fourfold or fivefold passaged viruses. This control was not possible for the double VPg Y-to-F mutants because of their extremely low titers. However, the stability of the mutation in these viruses is demonstrated by the fact that they continued to produce low virus titers and remained defective in forming plaques in semisolid medium, in contrast to the *wt* viruses and the recombinant rFMDV-C_{39}. The stability of the VPg deletion and insertion mutants is demonstrated by the number of their expressed VPg gene products (Fig. 3).

TABLE 1. Virus titers and [^{3}H]uridine incorporation into viral RNA of FMDV field isolates and VPg mutants[a]

Mutant	Titer (PFU/ml)	[^{3}H]uridine incorporation (cpm)
$O1_{Kaufbeuren}$	8 × 10^6	4,515
O_{Israel}	6 × 10^6	
$O1_{Murchin}$	4 × 10^6	
rFMDV-C_{39}	2 × 10^6	3,944
+VPg1+	8.5 × 10^5	3,505
ΔVPg1	7 × 10^5	1,990
VPg1F	4 × 10^5	
VPg2F	8.5 × 10^5	2,470
VPg3F	6 × 10^5	2,192
VPg1F/2F	8 × 10^4	
VPg1F/3F	5 × 10^4	
VPg2F/3F	1 × 10^5	1,456
ΔVPg2	ND[b]	

[a] Cellular RNA synthesis was blocked by the addition of 1 μg of actinomycin D per ml.
[b] ND, not determined.

Detection of VPg polypeptides. To investigate whether altered P3 polyprotein processing in the VPg mutants was the reason for their reduced viability, we analyzed the proteolytic cleavage products in vitro and in vivo using specific antisera directed against several P3-derived polypeptides.

Direct labeling and detection of VPg polypeptides are extremely difficult because of their small size, the lack of sulfur-containing amino acids, their basic hydrophilic character that results in their leaking from polyacrylamide gels during fluorography or fixation (5), and the rapid degradation of free VPg polypeptides in the infected cell (1, 6, 38). Therefore, we used an indirect method to study the proteolytic processing of the FMDV VPg precursor proteins by analyzing VPg fusions with the labeled neighboring polypeptide 3A. VPg is relatively stably linked to this membrane-anchoring protein (40), forming precursor polypeptides $3AB_1$, $3AB_{12}$, and $3AB_{123}$. Detection of these 3AB precursor proteins is much easier because of their methionine content and molecular masses, which range from 17 to 25 kDa.

Specific detection and assignment of these precursor products were possible because of the availability of two different antisera that, under the conditions used, strictly differentiate between polypeptide 3A (anti-E12) and polypeptide 3B (anti-EVPg) (41), allowing unequivocal detection of 3A- and 3B-specific bands on polyacrylamide gels. A third antiserum, specific for viral proteinase $3C^{pro}$ (anti-E20), which is responsible for processing of the whole P3 precursor polyprotein, was also used to investigate the correct processing of this polypeptide.

Polyprotein processing was studied by performing in vitro and in vivo protein synthesis over a course of time followed by immunoprecipitating the resulting processed products (Fig. 3). Analysis of cytoplasmic extracts of infected cells (Fig. 3, Cyto) in the control lanes shows that all mutants perform a host cell translation shutoff, since labeled host cell proteins were only weakly detectable.

In general, analysis of all immunoprecipitations of VPg polypeptides, synthesized either in vitro or in vivo, revealed a double-band pattern for all three VPgs (Fig. 3, products $3AB_1$, $3AB_{12}$, and $3AB_{123}$), whereas P3A did not give rise to this pattern. Since all of our Y-to-F amino acid exchange mutants also show a double-band formation for all three VPgs (Fig. 3, VPg1F, VPg2F, VPg3F, VPg1F/2F, VPg1F/3F, and VPg2F/3F), uridylylation of VPgs, as proposed formerly by Strebel et al. (41), cannot be the reason for this band duplication. In addition, we observed a successive appearance of the VPg precursor double bands in our kinetic experiments. Since VPg precursor bands with reduced levels of mobility appeared during infection earlier than their corresponding faster-migrating bands (Fig. 3, rFMDV-C_{39} in vitro and in vivo and +VPg1+ in vivo), secondary processing of a part of the VPg polypeptide seems to be the reason for this phenomenon. Experiments are in progress to further investigate the molecular basis of this observation.

Reduced viability of the VPg mutants is not due to altered viral polyprotein processing. Immunoprecipitations using antisera specific for proteins of the P3 region allowed detection of mature polypeptides 3A and $3C^{pro}$ and of their corresponding precursor polyproteins $3AB_1$, $3AB_{12}$, $3AB_{123}$, 3ABC, 3CD, and P3, as exemplified for *wt* virus ($O1_{Kaufbeuren}$) and recombinant *wt* virus (rFMDV-C_{39}) in Fig. 3 [O1K (wt), rFMDV-C_{39}]. In general, all VPg precursor polypeptides showed levels of mobility in polyacrylamide gels that are considerably lower than expected from their calculated molecular masses (Fig. 3). Retarded migration of the VPgs of FMDV was already reported by Strebel et al. (41) and Sangar et al. (38). This was also observed for poliovirus VPg (5, 43) and was attributed to the amino acid residue composition of this polypeptide.

Identical protein-processing patterns were always observed both in vitro and in vivo with *wt* virus ($O1_{Kaufbeuren}$), recombinant FMDV full-length cDNA clone-derived *wt* virus (rFMDV-C_{39}), and VPg mutant viruses (Fig. 3, in vitro and in vivo). 3B precursor proteins were not processed completely in vitro, resulting in VPg precursor bands even after an incubation time of 12 h (not shown). In comparison, viral P3 polyprotein processing in vivo was already complete 6 h postinfection (Fig. 3, rFMDV-C_{39}, ΔVPg1, and VPg1F in vivo).

Protein-processing patterns of all Y-to-F amino acid exchange mutant viruses were indistinguishable from the processing pattern obtained with *wt* virus, both in vitro and in vivo (Fig. 3, VPg1F, VPg2F, VPg3F, VPg1F/2F, VPg1F/3F, and VPg2F/3F).

Analysis of the VPg precursor proteins of mutant +VPg1+ revealed processing of P3 to be very similar to that observed for the *wt* virus, except for a fourth VPg precursor double band, corresponding to $3AB_{1234}$, which is clearly detectable in the immunoprecipitation reactions (Fig. 3, +VPg1+ in vitro and in vivo). This result clearly demonstrates (i) that the additional VPg1-coding region is stably integrated into the genome of this mutant, (ii) that the polyprotein of this mutant is correctly processed, and (iii) that it does not interfere with infective particle formation.

The processing pattern of VPg precursor proteins from the ΔVPg1 mutant was also found to be comparable to that for *wt* virus, except that a 33-kDa double band, corresponding to the $3AB_{123}$ precursor protein, did not appear in the immunoprecipitates as expected (Fig. 3, ΔVPg1 in vitro and in vivo). The weaker appearance of the $3AB_2$ bands (in comparison to the 3A and $3AB_{23}$ bands in the same lane) indicates a reduced cleavage between the two remaining VPgs in this mutant, possibly due to a slightly misfolded P3 precursor protein in this mutant.

The ΔVPg2 mutant showed strongly reduced levels of infectivity. Although cytopathic effects occurred at the same time as with *wt* virus (about 4 h postinfection), complete lysis of BHK cell monolayers was never observed. As shown in Table 1, infective virus particle production of this mutant is dramatically reduced. As a consequence of the reduced viability of this mutant, we were unable to produce enough virus particles to perform in vivo experiments. Proteolytic processing patterns of the ΔVPg2 precursor polypeptides in vitro (Fig. 3, ΔVPg2 in vitro) showed correct processing of the 3A, $3AB_{13}$, and $3C^{pro}$ species but only very weak $3AB_1$ corresponding bands, indicating a strongly reduced ability of this mutant to generate fully processed, single-VPg polypeptides. The fusion of VPg1 to the VPg3-coding region, therefore, seems to result in an unfavorable protease $3C^{pro}$ cleavage site in this mutant, which is most likely the reason for the observed reduced viability of the ΔVPg2 mutant virus.

In contrast to all other VPg mutants described here, the ΔVPg3 mutant showed changed, incomplete processing of the P3 precursor protein, a defect that is most probably responsible for its complete loss of infectivity. Experiments are in progress to further characterize the molecular basis of this observation, and results will be presented elsewhere.

The level of viral RNA synthesis correlates with the number of functional VPg molecules. Since all VPg mutants described here, especially the VPg Y-to-F amino acid residue exchange

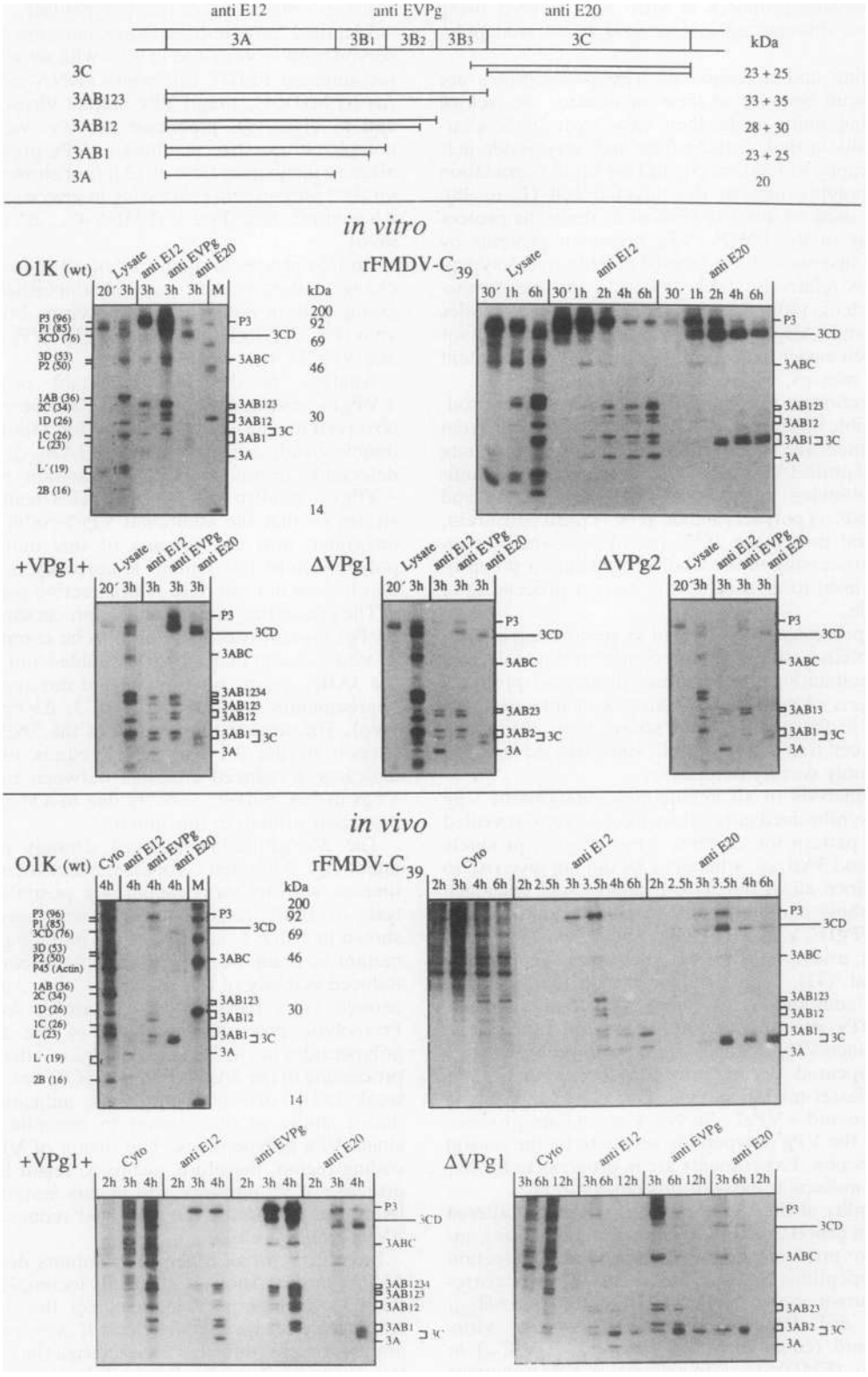
anti E12
anti EVPg
anti E20
3A
3B1
3B2
3B3
3C
kDa
3C
3AB123
3AB12
3AB1
3A
23 + 25
33 + 35
28 + 30
23 + 25
20
in vitro
O1K (wt)
Lysate
anti E12
anti EVPg
anti E20
20´ 3h
3h
3h
3h
M
kDa
200
92
69
46
30
14
P3 (96)
P1 (85)
3CD (76)
3D (53)
P2 (50)
1AB (36)
2C (34)
1D (26)
1C (26)
L (23)
L´ (19)
2B (16)
P3
3CD
3ABC
3AB123
3AB12
3AB1
3C
3A
rFMDV-C39
30´ 1h 6h
30´ 1h 2h 4h 6h
30´ 1h 2h 4h 6h
+VPg1+
20´ 3h
3h
3h
3h
3AB1234
3AB123
3AB12
ΔVPg1
3AB23
3AB2
ΔVPg2
3AB13
in vivo
O1K (wt)
Cyto
4h
4h
4h
4h
M
P45 (Actin)
rFMDV-C39
2h 3h 4h 6h
2h 2.5h 3h 3.5h 4h 6h
2h 2.5h 3h 3.5h 4h 6h
+VPg1+
2h 3h 4h
ΔVPg1
3h 6h 12h

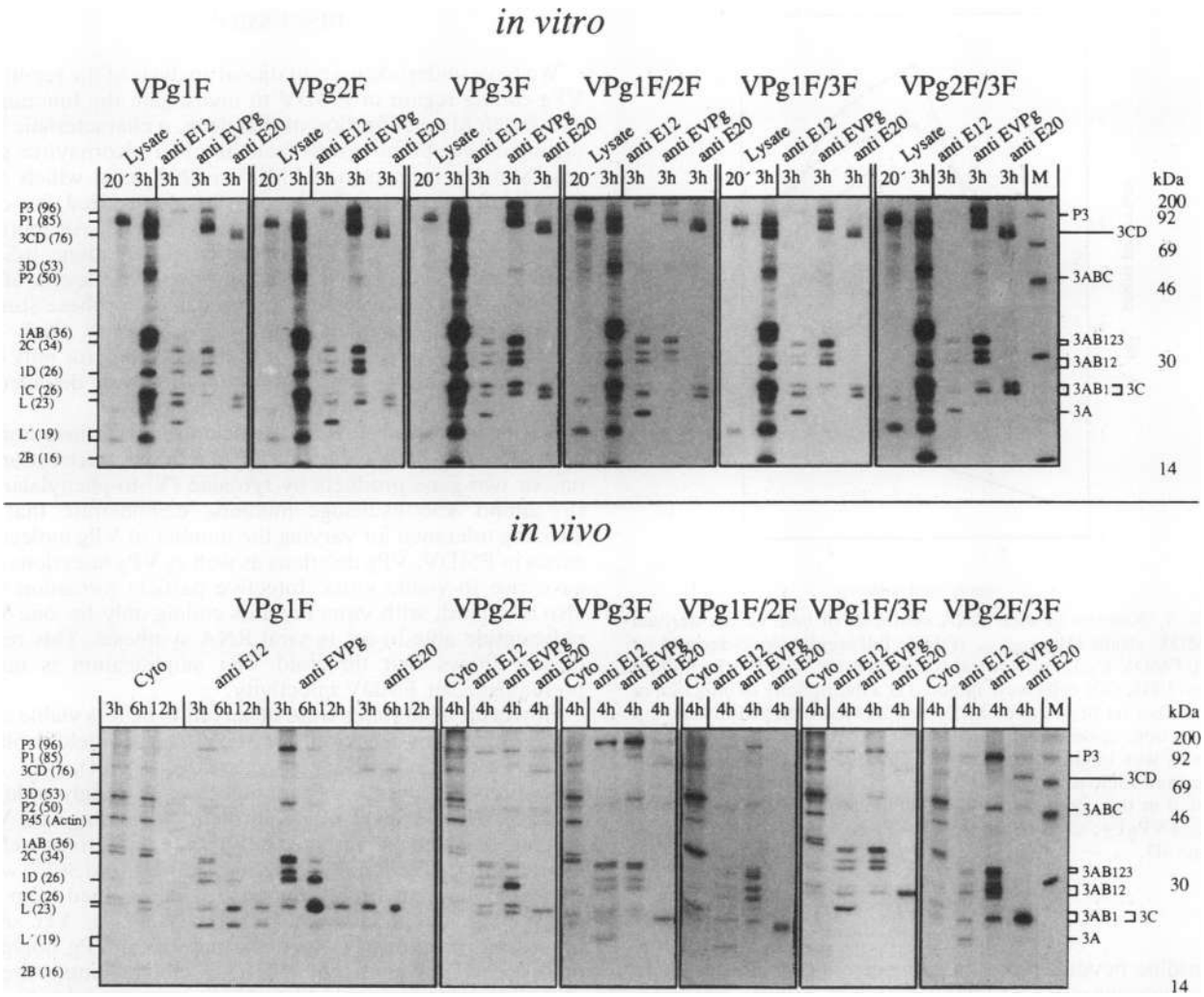

FIG. 3. In vitro and in vivo immunoprecipitation reactions of viral polypeptides derived from the P3 precursor polyprotein of field isolate-derived *wt* virus strain $O1_{Kaufbeuren}$ (O1K (wt), recombinant full-length clone-derived *wt* virus (rFMDV-C_{39}), and VPg mutant viruses. In vitro immunoprecipitations were performed after translation of synthetic viral RNA in a rabbit reticulocyte lysate in the presence of [^{35}S]methionine. At the indicated times, aliquots of the translation reaction mixtures were removed and further analyzed. In vivo immunoprecipitations were done after infection of BHK G21 cells with the individual viruses in the presence of [^{35}S]methionine. At the indicated times, infected cells were lysed and viral proteins were analyzed as described in detail in Materials and Methods. Viral polypeptide specific antisera were used to identify polypeptides 3A (anti E12), 3B or VPg (anti EVPg), and $3C^{pro}$ (anti E20). The corresponding viral precursor polyproteins $3AB_1$, $3AB_{12}$, $3AB_{123}$, 3ABC, 3CD, and P3 are also precipitated. As controls, complete labeled proteins of the reticulocyte lysates (Lysate) and cytoplasmic fractions of infected BHK G21 cells (Cyto) were analyzed, demonstrating viral polyprotein processing in vitro and in vivo and the virus-induced host cell protein synthesis shutoff. Several virus-derived proteins and cell-derived protein P45 (Actin), determined by immunoprecipitation reactions and calculated from their electrophoretic mobility, are marked. In general, all viruses examined showed identical processing products in vitro and in vivo. In vitro immunoprecipitation reactions were more sensitive than the reactions performed in vivo and therefore show fewer background bands of unspecific coprecipitated proteins. All 3AB precursor polypeptides and protease $3C^{pro}$ show a double-band pattern on SDS-polyacrylamide gels, while polypeptide 3A shows a single band only. A schematic drawing of polypeptide 3A, precursor polypeptides 3AB, and polypeptide $3C^{pro}$-derived processing products, visible on the gels, in combination with the corresponding specific antisera, is given above the figure. Molecular masses of proteins are indicated. For further details, see the text. M, marker proteins; 30', 30 min.

mutants, showed P3 precursor polyprotein processing very similar or identical to that of *wt* virus, altered viral polyprotein processing seemed unlikely to be the reason for the reduced virus particle formation of the mutants. To investigate possible effects at the transcriptional level, we measured RNA synthesis of the individual VPg virus mutants after infection. Because of the low titers of the double-VPg Y-to-F mutants, viral RNA synthesis was determined only for the more viable viruses. Figure 4 shows the results of [^{3}H]uridine incorporation studies into total viral RNA after infection. Cellular RNA synthesis was largely inhibited by actinomycin D (Fig. 4, +act.-D), while viral RNA synthesis became detectable approximately 1.5 to 3 h postinfection for *wt* ($O1_{Kaufbeuren}$), recombinant *wt* (rFMDV-C_{39}), and all VPg mutant viruses examined. Very similar results were obtained by Brown et al. (4) for FMDV strain SAT1. In general, about 3 h postinfection, viral RNA synthesis was found to be almost complete, as judged by a decreased incorporation of

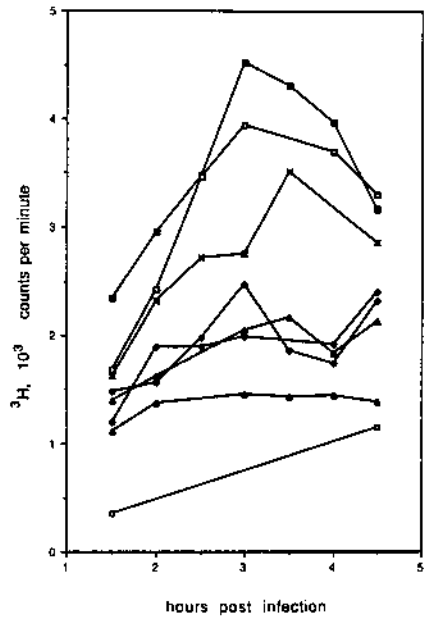

FIG. 4. Kinetics of viral RNA synthesis of field isolate-derived *wt* FMDV strain $O1_{Kaufbeuren}$ (O1K), full-length clone-derived *wt* virus (rFMDV-C_{39}), and several representative, viable VPg mutant viruses. BHK G21 cells were infected at a multiplicity of infection of 2 with either *wt* or mutant FMDV and labeled with [^{3}H]uridine 1 h postinfection, as described in Materials and Methods. Cellular RNA synthesis was inhibited by actinomycin D. As a control, levels of background radioactivity incorporated by uninfected cells are also indicated in this figure (+act.-D). Symbols: ■, O1K; □, rFMDV-C_{39}; x, +VPg1+; ◇, ΔVPg1; ◆, VPg2F; ▲, VPg3F; △, VPg2F/3F; ○, +act.-D.

[^{3}H]uridine beyond that time. In our experiments, a background incorporation of [^{3}H]uridine into cellular RNA, resulting in an additional increase in [^{3}H]uridine incorporation between 4 and 4.5 h postinfection (Fig. 4), was observed in all labeling reactions. This was probably due to an incomplete infection of the labeled cells at the low multiplicity of infection (2 PFU per cell) used in our RNA synthesis assay.

As observed for the virus titers (Fig. 2 and Table 1), RNA synthesis levels of the individual FMDV constructs can also be divided into three groups. The groups correspond to the number of VPg molecules encoded in the mutant virus that are able to promote viral RNA synthesis. One exception is the +VPg1+ mutant. The recombinant *wt* virus directed RNA synthesis at levels (rFMDV-C_{39}, 3,944 cpm at 3 h postinfection) comparable to those for field isolate-derived *wt* virus ($O1_{Kaufbeuren}$, 4,515 cpm at 3 h postinfection). The +VPg1+ mutant directed RNA synthesis at slightly reduced levels but is still comparable to *wt* viruses (3,505 cpm at 3.5 h postinfection). VPg mutant viruses encoding two VPg molecules were able to promote only significantly lower levels of RNA synthesis (between 1,990 and 2,470 cpm [^{3}H]uridine incorporation at 3 h postinfection). The third group is represented by VPg mutants that code for one VPg molecule that is able to act in viral RNA synthesis, resulting in very reduced RNA synthesis levels (1,456 cpm at 3 h postinfection) corresponding to nearly background values under the assay conditions used.

DISCUSSION

We have undertaken a mutational analysis of the repetitive VPg-coding region of FMDV to investigate the function of the threefold amplification of that gene, a characteristic that distinguishes aphthoviruses from all other picornavirus genera. Starting from cloned FMDV cDNA from which synthetic, infectious viral RNA could be synthesized, we constructed a whole set of VPg mutants (Fig. 1). All mutants were based on an improved FMDV cDNA clone (pSP65 FMDVpolyC) that shows markedly improved levels of infectivity. This construct was a prerequisite for these studies because FMDV mutants with very low virus titers (for example, the ΔVPg2 mutant or mutants coding for only one VPg able to promote viral RNA synthesis) were detected as viable only by using this clone.

Our results, derived from the deletion or the insertion of complete VPg gene copies or by functional inactivation of one or two gene products by tyrosine (Y)-to-phenylalanine (F) amino acid exchange mutants, demonstrate that an amazing tolerance for varying the number of VPg molecules exists in FMDV. VPg deletions as well as VPg insertions still gave rise to viable virus. Infective particle formation was also observed, with virus mutants coding only for one VPg polypeptide able to act in viral RNA synthesis. This result clearly shows that threefold VPg amplification is not a prerequisite for FMDV infectivity.

However, all mutants were observed to be less viable than the recombinant *wt* virus (rFMDV-C_{39}) or field isolate-derived *wt* viruses ($O1_{Kaufbeuren}$, $O1_{Murchin}$, O_{Israel}), and virus titers of several VPg mutants were strongly reduced (Fig. 2). At the level of polyprotein processing, all VPg mutants behaved similarly to the *wt* virus, in vitro as well as in vivo, after infection. Polypeptides 3A, 3B, and $3C^{pro}$ were correctly generated in all mutants, as determined from the analysis of the immunoprecipitations (Fig. 3). Yet some processing reactions between the individual VPg polypeptides occurred at a reduced rate in specific mutants. Altered processing of polypeptide 3A or $3C^{pro}$ was never observed in any of the VPg mutants. The band patterns of in vivo immunoprecipitations, less clear than those of the reactions performed in vitro (Fig. 3, in vitro and in vivo), are most likely due to (i) a more extended in vivo proteolytic degradation of viral proteins by various cellular proteases and (ii) the higher complexity of the in vivo antigen-antibody recognition conditions, which leads to coprecipitation of additional viral and cellular proteins involved in the membrane-bound picornavirus replication complex (30, 39, 40, 44), particularly polypeptide 2C.

An elongated life cycle, which could be caused by delayed viral polyprotein synthesis, delayed polyprotein processing in vivo (Fig. 3), or delayed kinetics of viral RNA synthesis (Fig. 4), as described for a poliovirus polypeptide 3AB mutant (14), was never observed for any of the VPg mutants. All mutants were observed to lyse the infected cells at the same time as the field-isolated and recombinant *wt* viruses (3 to 4 h postinfection; data not shown). Thus, a reduction in infectious particle generation must be the reason for the reduced efficiency of these VPg mutant viruses.

No obvious difference between the individual VPg molecules was observed with regard to promotion of viral RNA synthesis, indicating that all three VPgs act equally well in FMDV replication. The calculated number of infectious virus particles isolated per infected cell is approximately 50 from *wt* viruses, 10 from viruses that encode two functional VPg molecules, and only 1 to 2 from mutants, which encode

only one functional VPg. From these results we conclude that the number of VPg molecules that are competent in viral RNA synthesis and RNA linkage directly influences the amount of viral RNA synthesis and/or the number of correctly assembled infectious FMDV particles. The data suggest a direct role for VPg in FMDV RNA synthesis, possibly by acting as a primer for viral RNA synthesis, as originally postulated by Wimmer and coworkers (27) for poliovirus.

The simultaneous appearance of all 3A-VPg intermediates, which is also the case for the VPg Y-to-F mutants (Fig. 3), contradicts to a model of successive degradation from $3AB_{123}$ to 3A during RNA replication, generated either by the linkage of the terminal VPg to the newly synthesized RNA or by the elongation of the terminal VPg into viral RNA, followed by proteolytic cleavage from the precursor. Rather, proteolytic cleavage between individual VPgs seems to occur at random, and each of the three VPgs serves these functions equally and at the same time.

Our analysis of VPg mutants implies that cleaved, individual VPg polypeptides are necessary for FMDV viability. Two VPg molecules covalently linked to each other do not seem to function like single VPg molecules, as judged by the ΔVPg2 mutant, which is nearly defective in producing individual, free VPgs and therefore shows highly reduced levels of viability.

All data described in this report indicate that aphthovirus VPgs exert a direct gene dosage effect at the viral RNA synthesis level, with an optimum of three VPg molecules. However, explaining how triplet VPg amplification optimizes conditions for virus growth remains difficult. Major viral RNA synthesis was found to occur at 2 to 3 h postinfection in FMDV-infected BHK cells (Fig. 4) (4). At this time, the first VPg precursor products could be immunoprecipitated from the infected cells (Fig. 3). Also at this time, Brown et al. (4) observed a marked increase in newly synthesized FMDV particles in the infected cells. Degradation of the VPg precursors into completely processed, individual VPg molecules occurs only later in the infection cycle, namely, at 3 to 6 h postinfection (Fig. 3, in vivo). Thus, only very low amounts of free VPg molecules seem to be necessary for viral particle formation, an observation also described for poliovirus (40). Most of the VPg molecules are not used in virus particle formation and are rapidly degraded in the infected cell (1, 6, 38, 45). Tobin et al. (45) could show that the linkage of VPg to poliovirus RNA was highly influenced by the VPg concentration in vitro. The optimal concentration was approximately 50 μM. In FMDV, the threefold gene amplification serves most likely as a means of reaching a high VPg concentration, which may be either due to less efficient linking of VPg to the viral RNA or, more probably, due to the need for very effective RNA synthesis as a presupposition for the extremely short life cycle, only 2 to 3 h, of this virus group.

ACKNOWLEDGMENTS

We thank Klaus Strebel for preparing excellent FMDV-specific antisera and Laura Runkel and Michael Niepmann for help with the manuscript. M.F. is especially thankful to R. Rigg for helpful hints concerning in vivo viral RNA labeling and to N. Luz for several discussions about understanding VPg gene amplification.

Work at ZMBH was supported by grant BCT 381-5 from the Bundesministerium für Forschung und Technologie. Work at INIA was supported by the CICYT (grant BIO 88-0452-C05-03) and INIA (grant 05-7537).

REFERENCES

1. **Ambros, V., R. F. Pettersson, and D. Baltimore.** 1978. An enzyme activity in uninfected cells that cleaves the linkage between poliovirus RNA and the 5′ terminal protein. Cell **15:**1439–1446.
2. **Andino, A., G. E. Rieckhof, and D. Baltimore.** 1990. A functional ribonucleoprotein complex forms around the 5′ end of poliovirus RNA. Cell **63:**369–380.
3. **Beck, E., and K. Strohmaier.** 1987. Subtyping of European foot-and-mouth disease virus strains by nucleotide sequence determination. J. Virol. **61:**1621–1629.
4. **Brown, F., S. J. Martin, and B. Underwood.** 1966. A study of the kinetics of protein and RNA synthesis induced by foot-and-mouth disease virus. Biochim. Biophys. Acta **129:**166–177.
5. **Crawford, N. M., and D. Baltimore.** 1983. Genome-linked protein VPg of poliovirus is present as free VPg and VPg-pUpU in poliovirus-infected cells. Proc. Natl. Acad. Sci. USA **80:** 7452–7455.
6. **Dorner, A. J., P. G. Rothberg, and E. Wimmer.** 1981. The fate of VPg during in vitro translation of poliovirus RNA. FEBS Lett. **132:**219–223.
7. **Falk, M. M., P. R. Grigera, I. E. Bergmann, A. Zibert, G. Multhaup, and E. Beck.** 1990. Foot-and-mouth disease virus protease 3C induces specific proteolytic cleavage of host cell histone H3. J. Virol. **64:**748–756.
8. **Falk, M. M., F. Sobrino, and E. Beck.** Unpublished data.
9. **Flanegan, J. B., R. F. Petterson, V. Ambros, N. J. Hewlett, and D. Baltimore.** 1977. Covalent linkage of a protein to a defined nucleotide sequence at the 5′-terminus of virion and replicative intermediate RNAs of poliovirus. Proc. Natl. Acad. Sci. USA **74:**961–965.
10. **Flanegan, J. B., G. J. Tobin, M. S. Oberste, B. J. Marasco, D. C. Young, and P. S. Collis.** 1990. Mechanism of poliovirus negative-strand RNA synthesis and the self-catalyzed covalent linkage of VPg to RNA, p. 55–60. *In* M. A. Brinton and F. X. Heinz (ed.), New aspects of positive-strand RNA viruses. American Society for Microbiology, Washington, D.C.
11. **Flanegan, J. B., D. C. Young, G. J. Tobin, M. Merchant-Stokes, C. D. Murphy, and S. M. Oberste.** 1987. Mechanism of RNA replication by the poliovirus RNA polymerase, HeLa cell host factor, and VPg, p. 273–284. *In* M. A. Brinton and R. R. Rueckert (ed.), Positive strand RNA viruses. Alan R. Liss, Inc., New York.
12. **Forss, S., and H. Schaller.** 1982. A tandem repeat in a picornavirus. Nucleic Acids Res. **10:**6441–6450.
13. **Forss, S., K. Strebel, E. Beck, and H. Schaller.** 1984. Nucleotide sequence and genome organization of foot-and-mouth disease virus. Nucleic Acids Res. **12:**6587–6601.
14. **Giachetti, C., and B. L. Semler.** 1990. Molecular genetic analysis of poliovirus RNA replication by mutagenesis of a VPg precursor polypeptide, p. 83–93. *In* M. A. Brinton and F. X. Heinz (ed.), New aspects of positive-strand RNA viruses. American Society for Microbiology, Washington, D.C.
15. **Giachetti, C., and B. L. Semler.** 1991. Role of a membrane polypeptide in strand-specific initiation of poliovirus RNA synthesis. J. Virol. **65:**2647–2654.
16. **Grubman, M. J., and H. L. Bachrach.** 1979. Isolation of foot-and-mouth disease virus messenger RNA from membrane-bound polyribosomes and characterization of its 5′ and 3′ termini. Virology **98:**466–470.
17. **Harlow, E., and D. Lane.** 1988. Antibodies: a laboratory manual. Cold Spring Harbor Laboratory, Cold Spring Harbor, N.Y.
18. **Helenius, A., M. Marsh, and J. White.** 1982. Inhibition of semliki forest virus penetration by lysosomotropic weak bases. J. Gen. Virol. **58:**47–61.
19. **Higuchi, R., B. Krummel, and R. K. Saiki.** 1988. A general method of in vitro preparation and specific mutagenesis of DNA fragments: study of protein and DNA interactions. Nucleic Acids Res. **16:**7351–7367.
20. **Innis, M. A., D. H. Gelfand, and J. J. Sninsky.** 1990. PCR protocols: a guide to methods and applications. Academic Press, Inc., New York.
21. **King, A. M. Q., D. V. Sangar, T. J. R. Harris, and F. Brown.**

1980. Heterogeneity of the genome-linked protein of foot-and-mouth disease virus. J. Virol. **34**:627–634.
22. **Kingston, R. E.** 1987. Calcium phosphate transfection, unit 9.1, p. 1–4. *In* F. M. Ausubel, R. Brent, R. E. Kingston, D. D. Moore, J. G. Seidman, J. A. Smith, and K. Struhl (ed.), Current protocols in molecular biology–1987. John Wiley & Sons, Inc., New York.
23. **Kuhn, R. J., H. Tada, M. F. Ypma-Wong, B. L. Semler, and E. Wimmer.** 1988. Mutational analysis of the genome-linked protein VPg of poliovirus. J. Virol. **62**:4207–4215.
24. **Kuhn, R. J., and E. Wimmer.** 1987. The replication of picornaviruses, p. 17–51. *In* D. J. Rowlands, B. M. J. Mahy, and M. Mayo (ed.), The molecular biology of positive strand RNA viruses. Academic Press, Inc., New York.
25. **Lee, Y. F., A. Nomoto, B. M. Detjen, and E. Wimmer.** 1977. The genome-linked protein of picornaviruses. I. A protein covalently linked to poliovirus genome RNA. Proc. Natl. Acad. Sci. USA **74**:59–63.
26. **Melton, D. A., P. A. Krieg, M. R. Rebagliati, T. Maniatis, K. Zinn, and M. R. Green.** 1984. Efficient in vitro synthesis of biologically active RNA and RNA hybridization probes from plasmids containing a bacteriophage SP6 promoter. Nucleic Acids Res. **12**:7035–7056.
27. **Nomoto, A., B. Detjen, R. Pozzatti, and E. Wimmer.** 1977. The location of the polio genome protein in viral RNAs and its implication for RNA synthesis. Nature (London) **268**:208–213.
28. **Nomoto, A., N. Kitamura, F. Golini, and E. Wimmer.** 1977. The 5′-terminal structures of poliovirion RNA and poliovirus mRNA differ only in the genome-linked protein VPg. Proc. Natl. Acad. Sci. USA **74**:5345–5349.
29. **Paul, A., C.-F. Yang, S.-K. Jang, R. J. Kuhn, H. Tada, M. Nicklin, H.-G. Kräusslich, C.-K. Lee, and E. Wimmer.** 1987. Molecular events leading to poliovirus genome replication. Cold Spring Harbor Symp. Quant. Biol. **52**:343–352.
30. **Pincus, S. E., H. Rohl, and E. Wimmer.** 1987. Guanidine-dependent mutants of poliovirus: identification of three classes with different growth requirements. Virology **157**:83–88.
31. **Reuer, Q., C. U. T. Hellen, S.-K. Jang, C. Hölscher, H.-G. Kräusslich, and E. Wimmer.** 1990. Molecular and genetic analysis of events in poliovirus genome replication, p. 137–143. *In* M. A. Brinton and F. X. Heinz (ed.), New aspects of positive-strand RNA viruses. American Society for Microbiology, Washington, D.C.
32. **Reuer, Q., R. J. Kuhn, and E. Wimmer.** 1990. Characterization of poliovirus clones containing lethal and nonlethal mutations in the genome-linked protein VPg. J. Virol. **64**:2967–2975.
33. **Richards, O. C., and E. Ehrenfeld.** 1990. Poliovirus RNA replication. Curr. Top. Microbiol. Immunol. **161**:89–119.
34. **Rueckert, R. R.** 1990. Picornaviruses and their replication, p. 507–548. *In* B. M. Fields et al. (ed.), Virology, 2nd ed. Raven Press, New York.
35. **Rueckert, R. R., and E. Wimmer.** 1984. Systematic nomenclature of picornavirus proteins. J. Virol. **50**:957–959.
36. **Salas, M.** 1991. Protein-priming of DNA replication. Annu. Rev. Biochem. **60**:39–71.
37. **Sambrook, J., E. F. Fritsch, and T. Maniatis.** 1989. Molecular cloning: a laboratory manual, 2nd ed. Cold Spring Harbor Laboratory, Cold Spring Harbor, N.Y.
38. **Sangar, D. V., J. Bryant, T. J. R. Harris, F. Brown, and D. J. Rowlands.** 1981. Removal of the genome-linked protein of foot-and-mouth disease virus by rabbit reticulocyte lysate. J. Virol. **39**:67–74.
39. **Saunders, K., and A. M. Q. King.** 1982. Guanidine-resistant mutants of aphthovirus induce the synthesis of an altered nonstructural polypeptide, P34. J. Virol. **42**:389–394.
40. **Semler, B. L., C. W. Anderson, R. Hanecak, L. F. Dorner, and E. Wimmer.** 1982. A membrane-associated precursor to poliovirus VPg identified by immunoprecipitation with antibodies directed against a synthetic heptapeptide. Cell **28**:405–412.
41. **Strebel, K., E. Beck, K. Strohmaier, and H. Schaller.** 1986. Characterization of foot-and-mouth disease virus gene products with antisera against bacterially synthesized fusion proteins. J. Virol. **57**:983–991.
42. **Takeda, N., C.-F. Yang, R. J. Kuhn, and E. Wimmer.** 1987. Uridylylation of the genome-linked protein of poliovirus in vitro is dependent upon an endogenous RNA template. Virus Res. **8**:193–204.
43. **Takegami, T., R. J. Kuhn, C. W. Anderson, and E. Wimmer.** 1983. Membrane-dependent uridylylation of the genome-linked protein VPg of poliovirus. Proc. Natl. Acad. Sci. USA **80**:7447–7451.
44. **Takegami, T., B. L. Semler, C. W. Anderson, and E. Wimmer.** 1983. Membrane fractions active in poliovirus RNA replication contain VPg precursor polypeptides. Virology **128**:33–47.
45. **Tobin, G. J., D. C. Young, and J. B. Flanegan.** 1989. Self-catalyzed linkage of poliovirus terminal protein VPg to poliovirus RNA. Cell **59**:511–519.
46. **Toyoda, H., C.-F. Yang, N. Takeda, A. Nomoto, and E. Wimmer.** 1987. Analysis of RNA synthesis of type 1 poliovirus by using an in vitro molecular genetic approach. J. Virol. **61**:2816–2822.
47. **Wimmer, E.** 1979. The genome-linked protein of picornaviruses: discovery, properties and possible functions, p. 175–190. *In* R. Perez-Bercoff (ed.), The molecular biology of picornaviruses. Plenum Press, New York.
48. **Wimmer, E.** 1982. Genome-linked proteins of viruses. Cell **28**:199–201.
49. **Wimmer, E., R. J. Kuhn, S. Pincus, C.-F. Yang, H. Toyoda, M. Nicklin, and N. Takeda.** 1987. Molecular events leading to picornavirus genome replication. J. Cell Sci. Suppl. **7**:251–276.
50. **Young, D. C., D. M. Tuschall, and J. B. Flanegan.** 1985. Poliovirus RNA-dependent RNA polymerase and host cell protein synthesize product RNA twice the size of poliovirion RNA in vitro. J. Virol. **54**:256–264.
51. **Zibert, A., G. Maass, K. Strebel, M. M. Falk, and E. Beck.** 1990. Infectious foot-and-mouth disease virus derived from a cloned full-length cDNA. J. Virol. **64**:2467–2473.